Eksakta : Berkala Ilmiah Bidang MIPA
VOLUME 27 NO 06 2026, pp 1215-1228
ISSN : Print 1411-3724 — Online 2549-7464
DOI : https://doi.org/10.24036/eksakta/vol27-iss06/782

Eksakta
Berkala Ilmiah Bidang MIPA
http://www.eksakta.ppj.unp.ac.id/index.php/eksakta

Article

Characterization of Groundwater Flow in Porous Media Using the Self-Potential Method Based on Porous Pot ($CuSO_4$) Electrodes

Article Info

Article history :
Received October 16, 2026
Revised November 18, 2026
Accepted November 24, 2026
Published December 30, 2026
In Press

Keywords :
Groundwater,
porous pot electrodes,
self-potential,
streaming potential

Budy Santoso[1*], Imran Hilman Mohammad[1], Bambang Wijatmoko[1]

[1]Department of Geophysics, Faculty of Mathematics and Natural Science, Universitas Padjadjaran, Bandung, Indonesia

Abstract. An increase in shallow groundwater saturation within porous media primarily triggers slope instability, driven by declining effective stress as pore-water pressure rises. Continuous subsurface fluid monitoring is crucial for disaster mitigation but is frequently hindered by high commercial instrumentation costs. This study aims to characterize shallow groundwater flow utilizing the passive self-potential method with low-cost instrumentation. Its novelty lies in developing self-fabricated, non-polarizing porous pot ($Cu/CuSO_4$) electrodes using local calcined clay roof-tile waste as the ceramic membrane. This terracotta material possesses a microscopic pore network ensuring optimal ionic diffusion equilibrium, physically substituting expensive commercial sintered alumina. Laboratory calibration in an equipotential tank demonstrates a stable residual offset potential between 1.5 and 3.6 mV, well below the 5 mV operational threshold. Field mapping with a fixed-base configuration across 36 points in Hegarmanah Village proves high instrument sensitivity to streaming potential phenomena. The spatial distribution of electrical potential reveals critical hydrogeophysical heterogeneity. SP data successfully delineates the hydrogeological profile into dry slope (0–10 mV), moist transition (10–20 mV), saturated wet (>20 mV), and groundwater discharge zones featuring a sharp negative anomaly of −52.9 mV. These locally fabricated electrodes effectively map fluid seepage pathways, offering strong potential for landslide early warning systems.

This is an open acces article under the CC-BY license

This is an open access article distributed under the Creative Commons 4.0 Attribution License, which permits unrestricted use, distribution, and reproduction in any medium, provided the original work is properly cited. ©2026 by author.

Corresponding Author :
Budy Santoso
Department of Geophysics, Faculty of Mathematics and Natural Science,
Universitas Padjadjaran, Bandung, Indonesia
Email : santoso@unpad.ac.id

1. Introduction

The Shallow groundwater dynamics in porous media play an important role in controlling slope stability [1]. Rainfall infiltration can increase soil-water content and pore-water pressure, reduce matric suction and effective stress, and consequently decrease the shear strength of unsaturated or partially saturated soil [2]. These coupled hydrogeological and geotechnical processes are particularly critical in areas exposed to intense seasonal rainfall [3-4]. Effective assessment of these processes requires monitoring strategies capable of identifying spatial variations in subsurface water movement. While conventional instruments such as piezometers provide valuable point measurements, a limited number of monitoring locations may inadequately represent preferential seepage pathways or the spatial heterogeneity of shallow groundwater [5]. Furthermore, the high cost of commercial monitoring equipment often restricts the deployment of dense measurement networks, necessitating more accessible and reliable approaches.

The self-potential (SP) method is a passive geophysical technique that measures naturally occurring electrical potential differences at the ground surface. A primary source of SP signals is the electrokinetic (streaming-potential) effect, generated when pore water moves through porous materials and interacts with mineral surfaces [6-7]. Because it requires no external current source, the SP method is highly effective for investigating groundwater movement. However, its reliability strictly depends on the electrochemical stability of high-precision, non-polarizing electrodes to prevent distortions caused by contact polarization voltage (Nernst potential) [1], [8-9]. $Cu/CuSO_4$ porous-pot systems provide the necessary ionic contact between the internal electrolyte and the surrounding ground while limiting unwanted potential variations. Unfortunately, the substantial capital costs of commercial electrodes (e.g., sintered alumina or Ag/AgCl) limit the deployment of high-resolution spatial sensors, particularly in developing countries [10–12]. Previous work indicates that effective porous-pot electrodes can be constructed using simpler components, provided the porous plug and electrolyte characteristics are properly managed [8],[13-14].

The ceramic component is critical because its pore structure governs the ionic exchange between the internal electrolyte and the surrounding pore water. Research on clay-based porous ceramics demonstrates that porosity, pore-size distribution, and hydraulic permeability depend on raw-material composition and firing conditions [15]. Hydraulic conductivity is influenced not only by porosity but also by the shape, orientation, and connectivity of open pores [16]. These findings support the selection of fired-clay roof-tile fragments as a locally available, low-cost ceramic membrane. While these fragments may contain interconnected pores permitting ionic communication, their specific pore characteristics are sensitive to manufacturing history and should not be assumed identical to commercial ceramic filters or sintered alumina. Therefore, they must be rigorously evaluated through electrode calibration and field measurements.

To address the financial barriers to deploying dense SP measurement networks, this study fabricates $Cu/CuSO_4$ non-polarizing porous-pot electrodes using locally sourced fired-clay roof-tile waste [1],[13]. The primary objective is to evaluate the electrical stability of these self-fabricated electrodes and apply them to characterize the spatial distribution of shallow-groundwater-related SP anomalies at the Hegarmanah slope in Jatinangor [17]. Specifically, this study tests whether the locally fabricated electrode pair can achieve a residual offset potential below the operational threshold of 5 mV under equipotential laboratory conditions. Furthermore, field measurements across 36

observation points are conducted to determine if these electrodes can successfully resolve spatial contrasts, enabling the identification of relatively dry, moist-transition, and seepage-affected zones.

2. Material and Methods

2.1. Materials and Fabrication of Porous Pot Electrodes

The electrodes were fabricated from economical local components, comprising a transparent acrylic polymer pipe (1 inch in diameter) as the primary compartment, a fired clay roof-tile disc as the porous ion-exchange ceramic membrane, an oxygen-free pure copper rod as the electrode conductor, analytical-grade copper (II) sulfate pentahydrate ($CuSO_4 \cdot 5H_2O$) crystals, distilled water, and marine-grade waterproof epoxy resin [1]. The acrylic pipe was precisely cut, and its lower end was plugged with the fired clay roof-tile disc, which was securely attached using epoxy resin [1],[18]. The compartment tube was subsequently filled with a supersaturated $CuSO_4$ solution to maintain a stable ionic concentration. The copper rod was then inserted until fully submerged in the electrolyte solution, and the upper end of the tube was sealed using an airtight silicone sealant to prevent electrolyte leakage and evaporation.

It is important to note that the specific quantitative physical properties of the locally sourced fired clay roof-tile membranes, including absolute porosity, microscopic pore-size distribution, and fluid permeability, were not explicitly measured in this study. Therefore, no theoretical or assumed numerical values were assigned to these parameters. Instead, this limitation was addressed through empirical performance validation. The functional suitability of the ceramic membrane, particularly its ability to facilitate ionic communication between the internal electrolyte and the surrounding subsurface environment, was evaluated through laboratory offset-potential calibration and in-situ field sensitivity tests. These performance-based assessments provided experimental evidence of the electrode's operational functionality and suitability for self-potential (SP) measurements without relying on unverified physical parameters of the ceramic material.

2.2. Working Principle of the Self-Potential Method

The self-potential (SP) method is a passive geophysical technique that detects naturally occurring electrical potential differences in the subsurface without injecting electrical current from an external source. These potential anomalies primarily result from electrokinetic phenomena, particularly streaming potentials, generated within the electrical double layer when groundwater flows through porous media [13]. The working principle of the self-potential method is illustrated in Figure 1.

The operational principle of the SP method using porous pot electrodes involves measuring natural electrical potential differences through a pair of $Cu/CuSO_4$-based non-polarizing electrodes. The measurement configuration consists of a reference (base) electrode stationed at a fixed location and a moving (rover) electrode sequentially relocated across multiple measurement points. Both electrodes are connected to a Fluke 289 digital multimeter (DMM) with a high input impedance (>10 MΩ) to measure potential differences in millivolts (mV). The porous ceramic membrane facilitates ionic contact between the internal electrolyte solution and the surrounding soil pore water, while the $Cu/CuSO_4$ electrode system helps maintain a stable electrode potential.

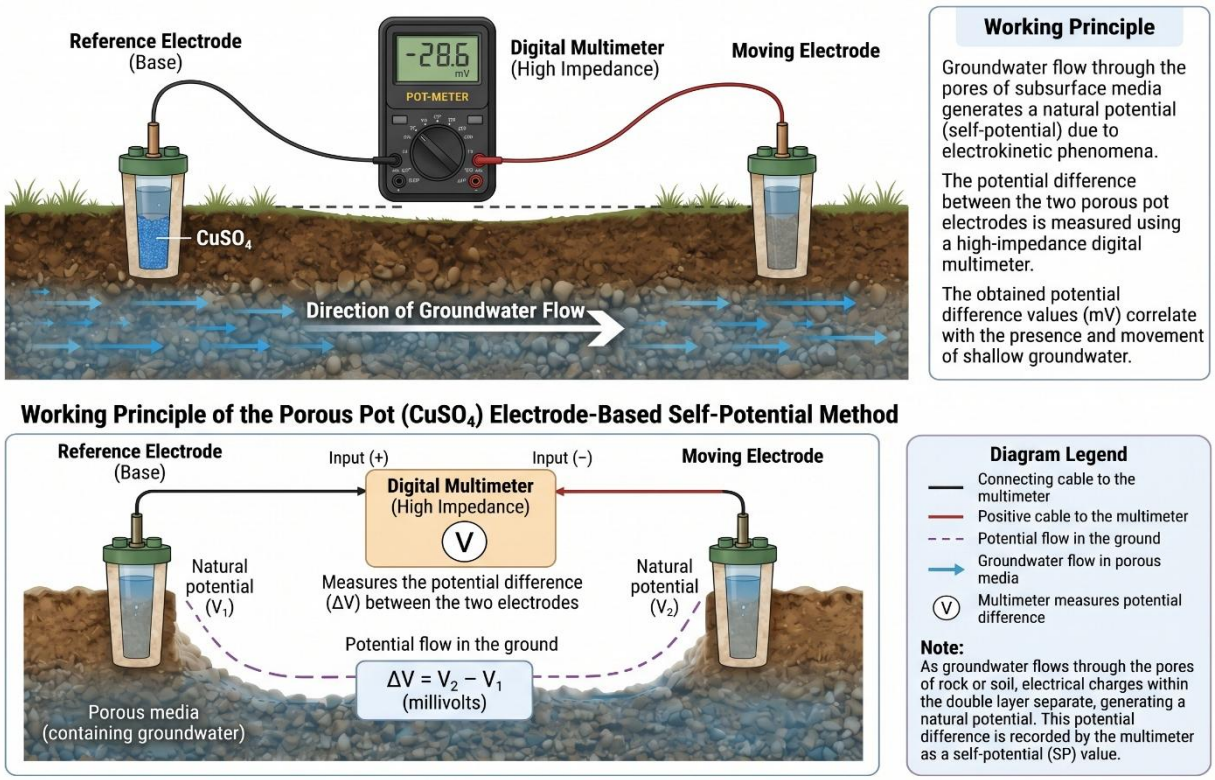


Figure 1. Mechanical Schematic and Working Principle of the Self-Potential Method

The movement of groundwater through soil or rock pores generates electrokinetic potentials (streaming potentials) through interactions between the moving fluid and mineral surfaces. These interactions produce electrical potential variations that can be detected by the SP electrode system. The measured potential differences are subsequently processed and spatially mapped to identify anomalies potentially associated with groundwater seepage pathways and shallow groundwater dynamics. Nevertheless, the interpretation of SP measurements must account for local geological conditions, subsurface material properties, and groundwater characteristics. This consideration is essential because the SP method measures electrical potential differences rather than directly determining groundwater discharge rates or flow directions.

The field measurement procedure using porous pot ($CuSO_4$) electrodes is illustrated in Figure 2. The procedure begins with equipment and accessory preparation, including checking the $CuSO_4$ electrolyte solution, inspecting electrode cables and electrical connections, and verifying the functionality of the digital multimeter. Initial electrode calibration is then performed by placing both electrodes in good electrical contact to assess their potential stability and ensure that the measured potential difference approaches 0 mV. If the readings remain unstable, the electrodes, electrical contacts, and electrolyte solution are inspected and corrective measures are undertaken before field measurements proceed.

Before the in-situ survey, the electrode pair undergoes laboratory calibration by immersing both electrodes in an equipotential tank designed to simulate conditions with negligible hydraulic and electrical potential gradients. This procedure is intended to determine the residual offset potential between the two electrodes [19-20]. The operational acceptance criterion requires the measured voltage difference between the electrode pair to be below 5.0 mV [1]. This threshold provides a practical reference for evaluating electrode compatibility and minimizing systematic errors associated with differences in electrode potentials during field measurements.

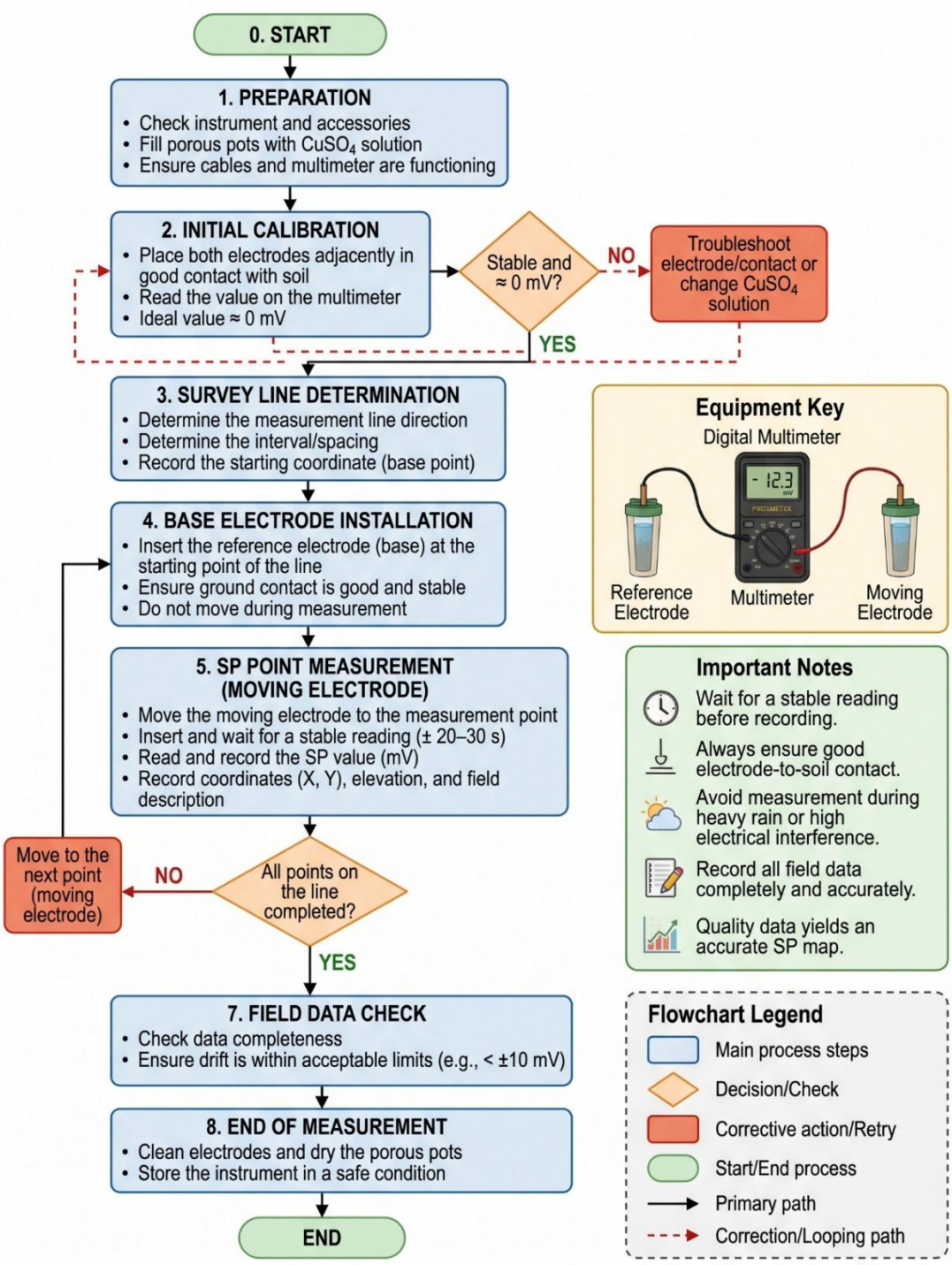


Figure 2. Flowchart of the Field Self-Potential Measurement Based on Porous Pot ($CuSO_4$) Electrodes

Following the laboratory calibration, the field survey layout is established by determining the measurement-line orientation, station spacing, and geographic coordinates of the initial reference electrode location. The SP survey employs the fixed-base measurement configuration [9], [21], in

which one porous pot electrode is permanently installed at a designated reference location (base station), while the second electrode serves as the moving electrode (rover electrode) and is sequentially relocated along the survey line. In this study, measurements were conducted at 36 sequential stations with a fixed spacing interval of 25 m between adjacent measurement points. At each measurement station, the rover electrode is placed in contact with the ground, and the potential difference relative to the fixed-base electrode is recorded using the high-input-impedance Fluke 289 digital multimeter. A stabilization period of two minutes is allowed before recording each voltage reading to minimize transient fluctuations and improve measurement consistency. The resulting dataset comprises spatially referenced electrical potential differences expressed in millivolts (mV), which are subsequently used to characterize subsurface SP anomalies.

The subsequent data-processing procedure involves signal quality control (QC) to minimize measurement errors associated with electrode polarization, electrical noise, and temporal instrument drift. The observed potential differences are referenced to the fixed-base station to maintain a consistent measurement reference throughout the survey. Where temporal instrument drift is identified, appropriate drift corrections are applied to the recorded measurements. The corrected SP dataset is then integrated with the corresponding geographic coordinates to facilitate spatial interpolation and the generation of two-dimensional SP potential distribution maps. These maps provide a basis for identifying and evaluating potential anomalies associated with groundwater seepage and subsurface fluid movement.

2.3. Data Processing

The linear relationship between the electrical potential field gradient (∇V) and the fluid pressure gradient (∇P) in the streaming potential phenomenon is expressed by the Helmholtz-Smoluchowski equation [3], [19]:

$$\nabla V = \frac{\varepsilon\, \zeta}{\eta\, \sigma} \nabla P \tag{1}$$

or expressed as a direct ratio:

$$\frac{\nabla V}{\nabla P} = \frac{\varepsilon_0 \varepsilon_r\, \zeta}{\eta\, \sigma} \tag{2}$$

where ∇V is the electrical potential gradient and ∇P is the fluid pressure gradient.

SP data processing begins with a baseline correction to normalize all data against the reference point (base electrode), ensuring that the potential values correspond to a uniform reference system. The equation to calculate the potential value at each observation point is expressed as follows:

$$SP_i = V_i - V_{ref} \tag{3}$$

where SP_i is the self-potential value at point i (mV), V_i is the measured potential difference at point i (mV), and SP_i is the potential difference at the reference electrode (mV).

If a systematic reading deviation over time is observed during field data acquisition caused by temperature fluctuations or changes in electrolyte characteristics a drift correction is applied. The drift correction value at time t is evaluated using the following equation:

$$D(t) = V_{ref}(t) - V_{ref}(t_0) \tag{4}$$

Under conditions of linear deviation, the drift is modeled using a linear regression equation:

$$D(t) = a + bt \tag{5}$$

where a is the initial constant and b is the rate of change of potential with respect to time. After accounting for the baseline and drift factors, the final electrical anomaly value is calculated using the following equation [22]:

$$SP_{i,corr} = V_i - V_{ref} - D(t_i) \quad (6)$$

Where $SP_{i,corr}$ is the pure potential value recorded after correction. The final data are then tabulated, visualized as one-dimensional graphs, and spatially interpolated using Surfer software to generate a 2D self-potential contour map to comprehensively delineate subsurface fluid flow vectors.

3. Results and Discussion

3.1. Empirical Site-Specific Calibration

Groundwater flow in porous media was investigated by integrating self-fabricated, nonpolarizing porous pot electrodes with a high-impedance digital multimeter. The primary sensors consisted of acrylic pipe bodies fitted at one end with porous ceramic discs fabricated from fired clay roof tiles, which served as ion-exchange membranes. Pure copper rods were immersed in saturated copper sulfate ($CuSO_4$) solutions contained within the acrylic tubes, forming electrode systems designed to maintain stable electrochemical potentials throughout the measurement process.

Before field deployment, the electrode pair underwent laboratory-scale calibration to evaluate its internal potential stability and assess the possibility of material-induced polarization. Both electrodes were immersed in a single water-filled container to simulate conditions without hydraulic or electrical potential gradients [13], [20]. The test results (Table 1) showed that the potential difference between the two electrodes (offset potential) was relatively stable, ranging from 1.5 to 3.6 mV. All measured values were below the standard operational threshold of 5 mV for geophysical surveys [22-23]. This low potential difference indicates that the internal electrochemical reactions between the pure copper rods and the $CuSO_4$ solutions in both electrodes had reached a relatively uniform equilibrium state. This condition demonstrates the relative electrochemical stability of the electrode system and minimizes the likelihood that variations in field measurements originate from internal potential differences between the electrodes. Consequently, the measurements are expected to provide a more reliable representation of subsurface streaming potential anomalies [13].

Table 1. Laboratory-Scale Offset Potential Calibration Results Based on Porous Pot Electrodes

Trial	Potential Value (mV)	Reference Potential (mV)	Remarks
1	2.6	0 - 5 mV *	Consistent with literature *
2	3.6	0 - 5 mV *	Consistent with literature *
3	1.5	0 - 5 mV *	Consistent with literature *
4	2.5	0 - 5 mV *	Consistent with literature *
5	1.7	0 - 5 mV *	Consistent with literature *
6	1.6	0 - 5 mV *	Consistent with literature *

*) [21,22]

Further validation tests were conducted in an open-field environment to evaluate the electrical responses of the electrodes to soil porosity heterogeneity and natural variations in moisture content. This field calibration phase involved measurements under different physical site conditions, ranging from relatively dry sloping terrain to depressions and drainage trenches characterized by water-saturated soils. The observed variations in self-potential (SP) signals indicate differences in electrical responses associated with local hydrogeological conditions. These findings are physically consistent with the electrokinetic potential mechanism explained by the cation-drag theory within the weathered soil matrix [1],[6].

The recorded electrical responses were strongly influenced by the degree of pore saturation and the velocity of fluid flow through the soil pores. In dry zones, potential values tended to exhibit relatively minor fluctuations around zero because of limited electrical charge transport. Conversely, in areas with high hydraulic gradients near drainage trenches, water movement can transport positive ions within the electrical double layer, resulting in relatively pronounced positive potential anomalies. These empirical observations provide an initial basis for developing an SP-based classification of soil moisture conditions, with potential ranges of 0–10 mV for dry soil, 10–20 mV for moist soil, and greater than 20 mV for water-saturated soil. This classification was subsequently used as an empirical approach to spatially map soil moisture distribution based on self-potential responses [24-25]. The physical classification derived from the field calibration results is presented in Table 2.

Table 2. Physical Classification of Field Electrical Calibration Results in Relation to Hydrogeological Conditions

Measurement Point	Potential Value (mV)	Field Condition	Hydrogeological Characteristics
SP-1	7.4	Slope	Dry
SP-2	10.5	Slope	Dry
SP-3	8.2	Slope	Dry
SP-4	2.4	Slope	Dry
SP-5	20.6	Adjacent to drainage channel	Water-saturated soil
SP-6	21.4	Adjacent to drainage channel	Water-saturated soil
SP-7	25.2	Adjacent to pond	Water-saturated soil
SP-8	26.9	Adjacent to pond	Water-saturated soil
SP-9	-25.2	Valley (topographic depression)	Water-saturated soil
SP-10	-20	Valley (topographic depression)	Water-saturated soil

3.2. Implementation of Porous Pot-Based Electrodes for the Identification of Groundwater Flow

Following laboratory testing and validation, the self-potential (SP) electrodes based on porous pot technology and using $CuSO_4$ as the electrolyte were deployed to characterize the natural electrical potential distribution associated with the occurrence and movement of shallow groundwater in porous media within the slope area of Hegarmanah Village, Jatinangor, Sumedang Regency, West Java. Field measurements were performed using the fixed-base method, in which one electrode was positioned at a relatively stable location as the reference (base electrode), while the second electrode was sequentially moved to each observation point to measure the potential difference relative to the reference electrode. This approach was adopted to ensure measurement consistency and facilitate comparisons among observation points throughout the survey area.

A total of 36 measurement points were distributed across the Hegarmanah slope to investigate spatial variations in SP values associated with soil moisture conditions, water-saturated zones, and shallow groundwater seepage pathways. The recorded data were subsequently processed through baseline normalization and drift correction to minimize systematic variations associated with the reference potential and temporal electrode drift, thereby isolating the electrokinetic potential anomalies of interest. The processed measurements were then compiled and analyzed to generate an SP potential distribution map, which was used to evaluate the capability of the self-fabricated porous pot electrodes to identify groundwater flow characteristics in a slope environment. An excerpt of the measured potential differences from the 36 observation points is presented in Table 3.

Table 3. Porous Pot-Based Potential Measurement Data Using the Self-Potential Method

Measurement Point	Longitude (Degrees)	Latitude (Degrees)	Measured Potential Value (mV)
SP 01	107.7736000	6.9186000	- 3.7
SP 02	107.7737331	6.9185819	- 3.2
SP 03	107.7738590	6.9185411	- 4.9
…	…	…	…
SP 35	107.7705497	6.9172982	-3.2
SP 36	107.7705739	6.9173182	-3.8

3.3. Qualitative Analysis Based on SP Graphs

The main survey line, comprising 36 measurement points across the Hegarmanah slope, revealed distinct spatial variations in self-potential (SP) values. The SP-01 to SP-16 segment exhibited relatively stable signals, ranging from −6.7 to +8.1 mV, reflecting predominantly unsaturated soil conditions with limited advective groundwater movement [1],[6]. Field data processing included quality control, correction for electrode reference potential, grouping according to survey lines, and graphical visualization. These procedures were performed to identify and characterize electrical anomalies along the slope. Based on the measurements presented in Table 3, two graphs were generated: the SP-01 to SP-16 survey line (Figure 3) and the SP-17 to SP-31 survey line (Figure 4).

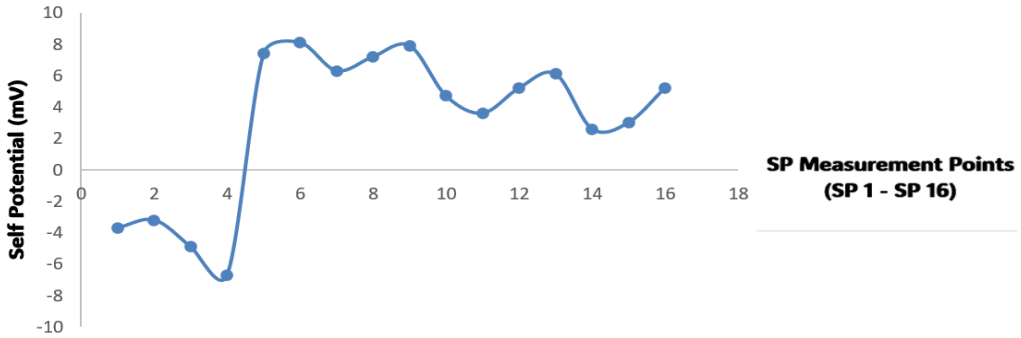


Figure 3. Graph of SP Values versus Measurement Points on the Dry Survey Line (SP-01–SP-16)

As shown in Figure 3, the SP values at points SP-01 through SP-04 fall within the negative range, decreasing from −3.7 mV to a minimum of approximately −6.7 mV at SP-04. Based on the site-specific physical calibration presented in Table 2, this range corresponds to relatively dry to transitional soil conditions, potentially indicating localized subsurface moisture variations. From SP-05 through SP-16, the curve rises and stabilizes within a positive range of 2.6 to 8.1 mV. According to the empirical classification established in Table 2, this segment is predominantly characterized by dry slope conditions and relatively low soil moisture content. The absence of pronounced potential anomalies suggests that this section is not significantly influenced by concentrated seepage or substantial groundwater movement. Overall, the relatively stable SP response along this segment indicates limited electrokinetic activity under predominantly unsaturated soil conditions.

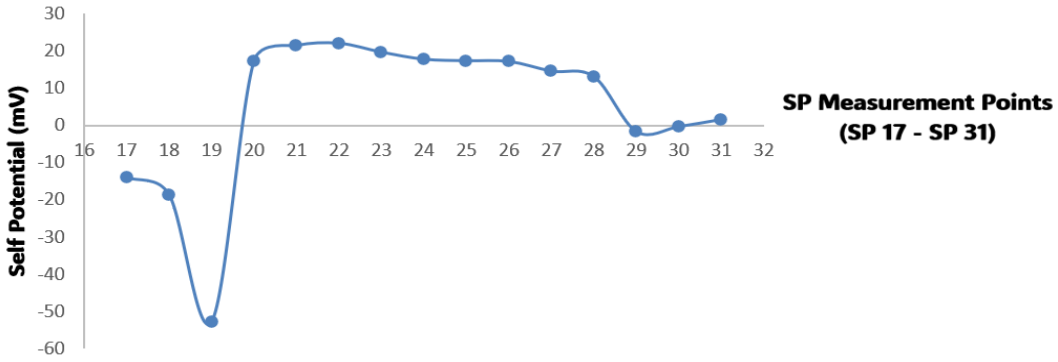


Figure 4. Graph of SP Values versus Measurement Points on the Wet Anomaly Survey Line (SP-17–SP-31)

In contrast, Figure 4 reveals substantially greater SP variations along the SP-17 to SP-31 segment, indicating pronounced spatial changes in subsurface hydrogeological conditions. A sharp decrease in potential occurs between SP-17 and SP-19, reaching a pronounced negative anomaly of −52.9 mV at SP-19. This potential deficit suggests a localized zone of groundwater convergence or preferential infiltration, where water originating from higher elevations may move downward and accumulate within a more permeable subsurface layer [26]. Rather than indicating static water accumulation alone, this negative anomaly may reflect active subsurface fluid migration associated with localized hydraulic gradients.

Following this pronounced negative anomaly, the SP curve rises sharply, reaching a positive peak of 22.1 mV at SP-21. The juxtaposition of negative and positive anomalies over a relatively short spatial distance indicates a contrasting electrokinetic response within the slope [27]. Although conventional SP interpretations commonly associate groundwater discharge with broad positive anomalies, the present findings exhibit a distinct negative–positive dipolar pattern.This pattern may be explained by topography-driven electrokinetic processes in heterogeneous subsurface media. Specifically, the negative trough at SP-19 may represent localized downward percolation of water into a permeable subsurface zone, whereas the adjacent positive peak at SP-21 may indicate the upward emergence of groundwater along a preferential seepage pathway or seepage face. This interpretation suggests a possible transition from localized infiltration and subsurface flow convergence to groundwater resurgence near the slope surface.

The pronounced potential contrast between SP-19 and SP-21 may also indicate subsurface hydraulic discontinuities associated with variations in lithology, permeability, or porosity. Such heterogeneity can influence groundwater migration and promote localized water accumulation above a relatively impermeable layer. Under these conditions, the retention of subsurface water may increase pore-water pressure and potentially contribute to the development of a slope instability zone or potential slip surface [21],[28]. However, the identification of an actual slip surface requires further verification through geological, geotechnical, or subsurface geophysical investigations.

Beyond the pronounced anomalies at SP-19 and SP-21, the SP values between SP-20 and SP-28 generally remain within a positive range of approximately 13–22 mV. Based on the empirical classification in Table 2, values exceeding 20 mV at SP-21 and SP-22 indicate water-saturated soil conditions associated with relatively active groundwater movement and pronounced streaming potential responses. Meanwhile, values ranging from 10 to 20 mV at SP-20 and SP-23 through SP-28 represent transitional moisture conditions that may be associated with localized seepage. These observations suggest that groundwater-related electrokinetic activity extends beyond the immediate locations of the principal negative and positive anomalies.

Finally, at points SP-29 through SP-31, the potential values decrease and stabilize near zero, within a range of approximately −2 to +2 mV. This response corresponds to relatively dry soil conditions with limited electrokinetic activity. The transition from pronounced positive anomalies to near-zero values indicates a spatial variation in subsurface moisture conditions and groundwater flow activity along the survey line.

3.4. Two-Dimensional Spatial Distribution Mapping of Shallow Groundwater Flow

Two-dimensional spatial mapping of self-potential (SP) distribution was performed by integrating geographic coordinates with field-measured electrical potential values using the Kriging spatial interpolation method to generate an SP contour map (Figure 5). The resulting map illustrates natural electrical potential variations ranging from approximately −55 to +23 mV. Based on the spatial distribution of the interpolated values, two principal anomaly zones with distinct hydrogeophysical characteristics were identified. The positive anomaly zone, with potential values ranging from approximately +20 to +25 mV around measurement points SP-20 to SP-21, indicates possible active shallow groundwater movement and seepage within the porous subsurface materials. In contrast, the negative anomaly zone, centered around SP-19 and reaching a minimum potential of −52.9 mV, represents a pronounced electrical anomaly potentially associated with localized groundwater convergence, preferential infiltration, or subsurface water accumulation. The marked contrast between these two zones reflects the heterogeneous nature of local hydrogeological conditions. However, the interpretation of groundwater flow directions and the identification of recharge and discharge zones cannot be established solely from SP potential values; they must also account for geological characteristics, topographic gradients, and supporting field-based hydrogeological observations.

The integration of the SP contour map with topographic elevation contours provides a spatial representation of the relationship between electrical potential anomalies and surface morphology. Directional vectors superimposed on the map illustrate the interpreted pathways of shallow groundwater movement, generally indicating flow from higher-elevation areas (recharge zones) toward lower-elevation areas (potential discharge zones). The spatial correspondence among electrical contour patterns, topographic gradients, and interpreted flow-vector orientations provides empirical support for the application of the porous pot-based SP method in tracing shallow groundwater flow pathways. Nevertheless, these vector orientations should be interpreted as inferred flow directions rather than direct measurements of groundwater velocity or hydraulic flow. The observed spatial correspondence also supports the potential of the self-fabricated electrodes to resolve hydrogeophysical variations across the study area. Locally adapted, low-cost geophysical sensors can provide reliable results for mapping complex tropical terrains when appropriate electrochemical stability and calibration procedures are maintained [10]. However, a direct assessment of their accuracy relative to commercial instruments requires comparative measurements under equivalent field conditions.

From a hydrogeophysical and geotechnical perspective, the presence of shallow groundwater seepage and subsurface water accumulation within a slope requires particular attention because increasing soil saturation can reduce matric suction and elevate pore-water pressure. These changes may reduce effective stress and soil shear strength, thereby compromising slope stability and increasing the potential for landslides [3],[28-30]. Accordingly, the area surrounding measurement points SP-19 through SP-21 represents a priority zone for further investigation to establish the relationship between SP anomalies, soil moisture distribution, groundwater seepage, and potential slope instability. In particular, the juxtaposition of pronounced negative and positive anomalies may indicate contrasting subsurface hydraulic conditions that warrant additional geological and geotechnical verification.

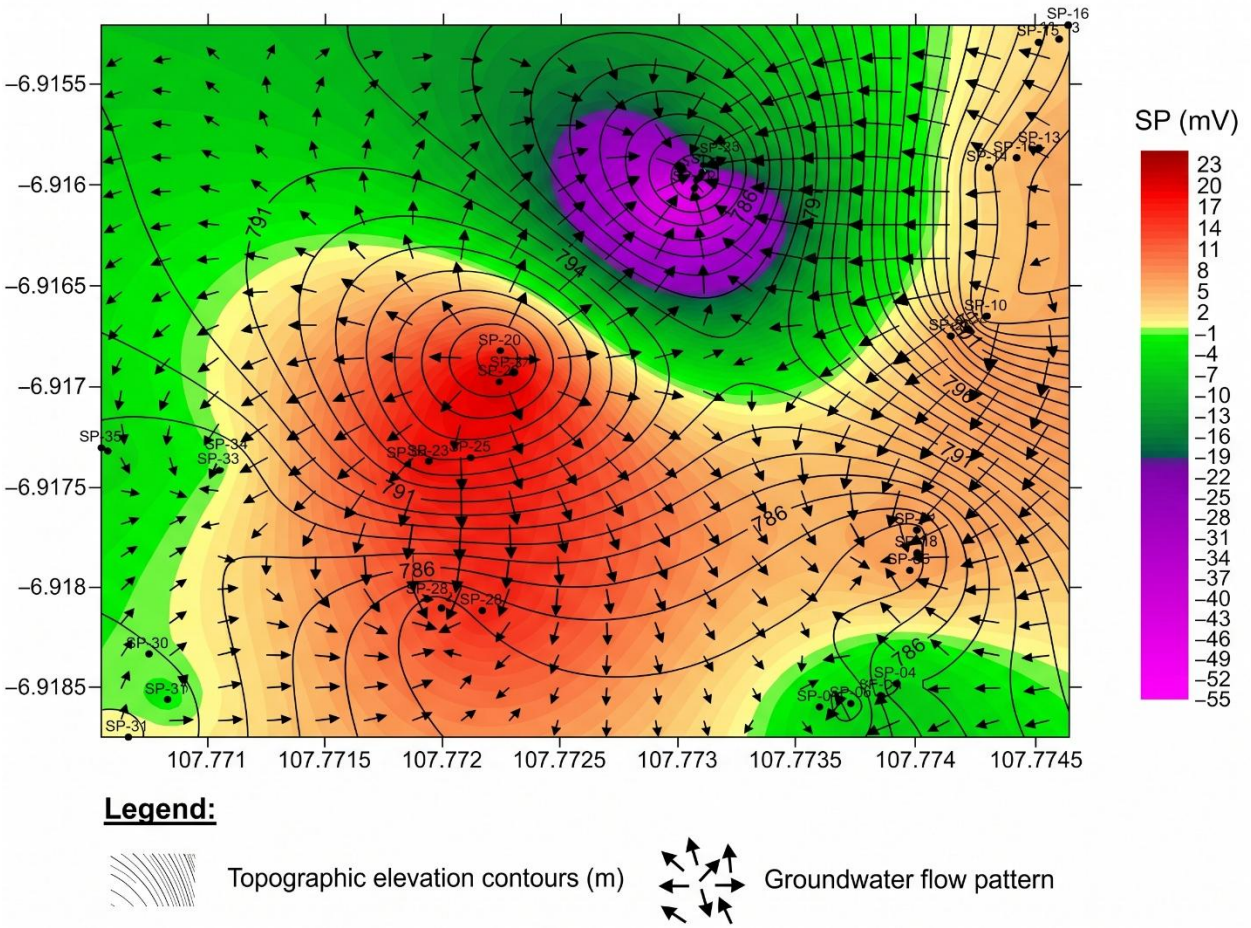


Figure 5. Self-potential (SP) distribution contour map illustrating the patterns and directional vectors of shallow groundwater flow.

Overall, the findings demonstrate the potential of the porous pot-based SP method as a relatively low-cost geophysical approach for the preliminary identification and spatial mapping of shallow groundwater seepage pathways. Its sensitivity to spatial variations in natural electrical potential provides a basis for monitoring changes in subsurface hydrogeological conditions. Further development through periodic SP measurements, integration with Internet of Things (IoT)-based monitoring sensors, and simultaneous measurements of relevant hydrogeological and geotechnical parameters could support the development of a more affordable and responsive landslide early warning system [25],[29],[31-32]. The area around SP-19 through SP-21 is therefore recommended as a priority location for subsequent field verification and periodic monitoring, particularly during periods of high rainfall.

4. Conclusion

The application of self-fabricated porous pot ($Cu/CuSO_4$) electrodes using the Self-Potential (SP) method successfully characterized shallow groundwater dynamics in porous media. Field measurements in Hegarmanah Village quantitatively delineated the subsurface hydrogeology into four distinct zones based on streaming potential responses: a dry slope (0–10 mV), a moist transition (10–20 mV), a saturated wet zone (20 mV), and a critical groundwater discharge zone. The spatial mapping effectively identified active fluid accumulation and seepage pathways, prominently marked by a sharp

negative anomaly of −52.9 mV. These empirical indicators confirm that the low-cost SP instrumentation is highly sensitive to variations in groundwater saturation. By accurately localizing subsurface seepage vectors that can increase pore water pressure and threaten soil shear strength, this method provides a reliable geophysical approach to support preliminary assessments and the development of early warning systems for slope instability.

References

[1] Ahmad, N., Hussain, S., and Ali, M. (2023). Development of porous medium sensors for water detection. *Sensors, 23* (18), 7892.

[2] Bucher, K., et al. (2023). Modeling the temporal evolution of streaming potentials during controlled infiltration. *Geophysical Journal International, 235*(1), 345–360.

[3] Bai, L., Huo, Z., Zeng, Z., Liu, H., Tan, J., and Wang, T. (2021). Groundwater flow monitoring using time-lapse electrical resistivity and self-potential data. *Journal of Applied Geophysics,* 193, 104411.

[4] Bolève, A., et al. (2021). Electrokinetic coupling in unsaturated slopes: Laboratory and field constraints. *Water Resources Research, 57*(3), e2020WR028741.

[5] Chen, H., Wu, Y., and Zhang, Q. (2024). Soil moisture monitoring using low-cost electrical sensors. *Environmental Research,* 242, 117485.

[6] Corwin, R. F. (1990). The self-potential method for environmental and engineering applications. In S. H. Ward (Ed.), *Geotechnical and Environmental Geophysics* (Vol. 1, pp. 127–145). Society of Exploration Geophysicists.

[7] Revil, A., Finizola, A., and Gresse, M. (2023). Self-potential as a tool to assess groundwater flow in hydrothermal systems: A review. *Journal of Volcanology and Geothermal Research*, 437, 107788.

[8] Comeau, M. J., Ueding, S., and Becken, M. (2024). Long-term stability, noise, and temperature sensitivity of modular porous-pot electrodes designed for geophysical and geotechnical applications. *Earth and Space Science, 11*(2), e2023EA003327.

[9] Deng, Y., et al. (2021). Effects of terracing on hydrological connectivity and soil moisture in mountain catchments. *Journal of Hydrology*, 594, 125951.

[10] Hassan, A., Ali, R., and Mahmood, T. (2024). Resistive sensing for shallow groundwater detection. *Water Resources Management*, 38, 3121–3135.

[11] Hu, K., Huang, Q., Tang, M., Xue, L., and Han, P. (2024). Self-potential variations associated with the slip of Huangnibazi Landslide. *Journal of Applied Geophysics*, 220, 105275.

[12] Vaudelet, P., et al. (2024). Groundwater flow paths using combined self-potential, electrical resistivity, and induced polarization signals. Geophysical *Journal International, 239*(2), 798–820.

[13] Zhang, Y., & Wang, H. (2023). Machine learning-enhanced self-potential tomography for landslide early warning systems. *Journal of Applied Geophysics*, 215, 105123.

[14] Omoniyi, Oluwole A., Ali A. Salifu, John D. Obayemi, Oluwaseun K. Oyewole, Pierre-Marie Nigay, Omololu Akin-Ojo, and Winston O. Soboyejo. 2022. Effects of Sintering Temperature on the Filtration and Mechanical Properties of Ceramic Water Filters. *Cogent Engineering 9* (1): 2119536.

[15] Elmore, A. Curt, William Fahrenholtz, L. G. Glauber, and Allison N. Sperber. 2011. Calculation of Ceramic Pot Filter Hydraulic Conductivity Using Falling-Head Data. *Water Science and Technology: Water Supply 11* (3): 358–63.

[16] Smith, J. R., et al. (2022). High-density self-potential monitoring of transient groundwater flow in unstable slopes. *Water Resources Research, 58*(4), e2021WR031122.

[17] García-Fernández, M., Martínez, J., and Pérez, A. (2023). Advances in groundwater detection using electrical methods. *Water, 15*(4), 685.

[18] Chavanne, X., & Frangi, J. P. (2017). Autonomous sensors for measuring continuously the moisture and salinity of a porous medium. *Sensors (Basel, Switzerland)*, *17*(5), 1094.
[19] Ivanova, I., Dimitrov, M., and Petrov, P. (2025). Soil moisture estimation using electrical conductivity sensors. *Environmental Monitoring and Assessment*, 197, 102.
[20] Jiang, Z., et al. (2022). A depth-resolved hydro-mechanical triggering model for dynamically determining the sliding surface of shallow landslides. *Water Resources Research, 58*(12), e2022WR032716.
[21] Li, D.-Q., Kang, Q., Yan, K., He, J.-P., and Liu, Y. (2026). A dynamic multi-objective inversion framework for seepage parameters based on monitoring data: Case study of an earth-rockfill dam. *Journal of Hydrology,* 669, 135064.
[22] Santoso, B., Hendarmawan, and Rosandi, Y. (2024). Study of groundwater flow patterns in landslide prone areas using the Self Potential Method. *IOP Conference Series: Earth and Environmental Science,* 1373, 012012.
[23] Heinz, E., et al. (2025). The impact of soil conservation practices on subsurface water flow and agricultural resilience. *Soil and Tillage Research,* 246, 106312.
[24] Wang, Y., Li, X., and Zhao, J. (2023). Monitoring water content in porous media using electrical resistance methods. *Measurement,* 214, 112810.
[25] Zhao, L., Huang, J., and Li, W. (2022). Soil electrical conductivity response to water content variation. *Catena,* 214, 106248.
[26] Liang, M.-C., Chen, H.-E., Tfwala, S. S., Lin, Y.-F., and Chen, S.-C. (2023). The application of wireless underground sensor networks to monitor seepage inside an earth dam. *Sensors*, 23, 3795.
[27] Loconsole, D., Elia, M., Conversa, G., Bonasia, A., et al. (2025). Soil moisture sensing technologies: Principles, applications and challenges. *Agronomy, 15*(12), 2788.
[28] Singh, R., Kumar, A., and Sharma, P. (2023). Electrical conductivity as a proxy for soil moisture assessment. Journal of Applied Geophysics, 210, 104997.
[29] Martins-Gomes, A., et al. (2023). Evaluation of interface phenomena in self-potential surveys for groundwater exploration. *Near Surface Geophysics, 21*(5), 455–472.
[30] Qi, Y., and Wu, X. (2022). Comprehensive geophysical monitoring of slope stability using electrical and seismic methods. *Landslides, 19*(8), 1955–1971.
[31] Olabode, O. P., Lim, H. S., and Ramli, M. H. (2022). Geophysical and geotechnical evaluation of landslide slip surface in a residual soil for monitoring of slope instability. *Earth and Space Science,* 9, e2022EA002248.
[32] Saco, P. M., et al. (2021). Degradation processes and the reduction of soil capacity to buffer hydro-climatic extremes. *Science of the Total Environment,* 765, 142721.